DUAL RIDGELET FRAME CONSTRUCTED USING BIORTHOGONAL WAVELET BASIS

Tan Shan, Xiangrong Zhang, and Licheng Jiao, Senior Member, IEEE

Institute of Intelligent Information Processing, Xidian University, Xi'an, 710071, China

ABSTRACT

A new system called dual ridgelet frame is introduced in this paper. The construction of the dual ridgelet frame starts with a dual frame constructed using biorthogonal wavelet basis in Radon domain, and then, the image of the resulting dual frame under an isometric map from Radon domain to $L^2(R^2)$ is a dual frame again, and we call it dual ridgelet frame. The dual ridgelet frame can be thought of as an extension of the notion of orthonormal ridgelet. And it provides a more flexible and effective tool for image analysis and processing application. Also, the high performance of the dual ridgelet frame for image denoising is demonstrated experimentally.

1. INTRODUCTION

To represent signal parsimoniously is fundamental to many applications such as image analysis and processing task. It is well known that the separable wavelet system in two dimensions fails at dealing with the edge of images effectively. In other words, the nonlinear approximation ability of separable wavelet system is not satisfying when one uses it to represent two-dimension functions smooth away from straight and curve singularity. Much research work has been done to find better mathematical tools than wavelet system [1] [2] [3]. Candès introduced the notion of ridgelet system in 1998 [3]. In a following paper [4], Donoho developed a new orthonormal system in $L^2(R^2)$, called orthonormal ridgelet. Both ridgelet system and the orthonormal ridgelet can represent nearly optimally the two-dimension functions smooth away from straight singularity. For convenience below, by the terms ridgelet analysis we mean both systems introduced by Candès and by Donoho. The optimal nonlinear approximation ability of ridgelet analysis is obtained from the fact that the ridgelet analysis first convert straight singularity into point singularity by Radon transform, and then, the resulting point singularity is dealt with wavelet system. The construction of orthonormal ridgelet has to make use of two special property of Meyer wavelet, namely, the closure property under reflection about the origin in the ridge direction $\psi_{j,k}(-t)=\psi_{j,1-k}(t)$, and closure property under translation by half a cycle in the angular direction $w^{\varepsilon}_{i,l}(\theta+\pi)=w^{\varepsilon}_{i,l+2^{i-1}}(\theta)$. Of the two special closure properties, the one under reflection does not hold for most orthonormal wavelet families, such as Daubechies compactly supported wavelet. In other words, only few kinds of wavelet can be made use of to construct orthonormal ridgelet. At the cost of losing the orthonormality, one can substitute other dominant wavelet for the Meyer wavelet, then, a tight frame can be obtained [5]. By this methodology, we constructed a tight frame with frame bound 1 in paper [6], where the associated proofs was given and the ability of the resulting tight frame for image denoising was investigated also. And we call the constructed tight frame with frame bound 1 ridgelet frame. The ridgelet frame can be considered as a natural extension of orthonormal ridgelet.

In this paper, we furthermore extend the ridgelet frame to a more general situation, i.e., dual frame. Instead of using orthonormal wavelet, we construct a dual frame in $L^2(R^2)$ by using biorthogonal wavelet basis. We call this kind of dual frame as dual ridgelet frame.

This paper is organized as follows. In Section 2, the construction of dual ridgelet frame is proposed and the associated proofs are given. Then, in section 3, we investigate the performance of the dual ridgelet frame for image denoising, and the denoising results are compared with that of algorithms based on wavelet both visually and in terms of the PNSR. Finally, concluding remarks are given in Section 4.

2. DUAL RIDGELET FRAME

It is well known that there exists an isometric map from Radon domain $\Re$ to spatial domain $L^2(R^2)$. To construct a dual frame, we first construct a dual frame in Radon domain using biorthogonal wavelet basis. Then, under the isometric map, the image of the resulting dual frame in Radon domain is also a dual frame in $L^2(R^2)$.

Let $\{\psi_{j,k},\tilde{\psi}_{j,k}: j,k\in Z\}$ and $\{\omega_{i,l},\tilde{\omega}_{i,l}: i,l\in Z\}$ be two biorthogonal wavelet systems in $L^2(R)$. For convenience below, we denote the former one by ψ and $\tilde{\psi}$. Analogously, we denote the periodization version of the later one on $[0,2\pi)$ by $\omega:=\omega^{per}_{i,l}(\theta)$ and $\tilde{\omega}:=\tilde{\omega}^{per}_{i,l}(\theta)$. Obviously, the tensor product $\{w''_{\lambda}=\psi\otimes\omega:\lambda\in\Lambda\}$ and

$\{\tilde{w}''_\lambda = \tilde{\psi} \otimes \tilde{\omega} : \lambda \in \Lambda\}$ is a biorthogonal system for $L^2(R \otimes [0,2\pi))$, here Λ is the correlative index set.

Define orthoprojector $P_{\Re}$ from $L^2(R \otimes [0,2\pi))$ to Radon domain by

$$(P_{\Re}F)(t,\theta) = (F(t,\theta) + F(-t,\theta+\pi))/2 \quad (1)$$

where $F \in L^2(R \otimes [0,2\pi))$.

Let $w'_\lambda := 2\sqrt{\pi}w''_\lambda$ and $\tilde{w}'_\lambda := 2\sqrt{\pi}\tilde{w}''_\lambda$. Then, applying $P_{\Re}$ on w'_λ and $\tilde{w}'_\lambda$, we obtain

$$w_\lambda := P_{\Re}(w'_\lambda) = (\frac{I + T \otimes S}{2})w'_\lambda = 2\sqrt{\pi}P_{\Re}(w''_\lambda) \quad (2)$$

$$\tilde{w}_\lambda := P_{\Re}(\tilde{w}'_\lambda) = (\frac{I + T \otimes S}{2})\tilde{w}'_\lambda = 2\sqrt{\pi}P_{\Re}(\tilde{w}''_\lambda) \quad (3)$$

where operator T is defined by $(Tf)(t) = f(-t)$ and operator S is defined by $(Sg)(\theta) = g(\theta+\pi)$.

We will show that w_λ and $\tilde{w}_\lambda$ is a dual frame in $\Re$.

Lemma 2.1. Both w_λ and $\tilde{w}_\lambda$ are complete in Radon domain $\Re$.

Proof. For $\forall F \in \Re$, it is obvious that $F \in L^2(R \otimes [0,2\pi))$ and we have $F = P_{\Re}F$ due to the definition of $P_{\Re}$. Then, we have

$$\begin{aligned} F &= \sum_{\lambda\in\Lambda} <\mathrm{F}, w''_\lambda> w''_\lambda = \sum_{\lambda\in\Lambda} <\mathrm{F}, w''_\lambda> P_{\Re}(\frac{1}{\sqrt{2\pi}} w'_\lambda) \\ &= \frac{1}{\sqrt{2\pi}} \sum_{\lambda\in\Lambda} <\mathrm{F}, w''_\lambda> w_\lambda \end{aligned} \quad (4)$$

$$\begin{aligned} F &= \sum_{\lambda\in\Lambda} <\mathrm{F}, \tilde{w}''_\lambda> w''_\lambda = \sum_{\lambda\in\Lambda} <\mathrm{F}, \tilde{w}''_\lambda> P_{\Re}(\frac{1}{\sqrt{2\pi}} w'_\lambda) \\ &= \frac{1}{\sqrt{2\pi}} \sum_{\lambda\in\Lambda} <\mathrm{F}, \tilde{w}''_\lambda> w_\lambda \end{aligned} \quad (5)$$

Lemma 2.2. For $\forall F \in \Re$,

$$< w''_\lambda, F > = <(\mathrm{T} \otimes \mathrm{S})w''_\lambda, F> \quad (6)$$

$$< \tilde{w}''_\lambda, F > = <(\mathrm{T} \otimes \mathrm{S})\tilde{w}''_\lambda, F> \quad (7)$$

Proof. It is easy to obtain the relation (6) by computing both $< w''_\lambda, F >$ and $<(\mathrm{T}\otimes\mathrm{S})w''_\lambda, F>$ respectively. Analogously, (7) holds also.

Lemma 2.3. For $\forall F \in \Re$,

$$< w''_\lambda, F > = 2\sqrt{\pi}[w_\lambda, F] \quad (8)$$

$$< \tilde{w}''_\lambda, F > = 2\sqrt{\pi}[\tilde{w}_\lambda, F] \quad (9)$$

Proof.

$$\begin{aligned} [w_\lambda, F] &= \frac{1}{4\pi}\int_0^{2\pi}\int_{-\infty}^{\infty} W_\lambda(t,\theta)\bar{F}(t,\theta)dtd\theta \\ &= \frac{1}{4\pi} \times 2\sqrt{\pi} \int_0^{2\pi}\int_{-\infty}^{\infty} \frac{w''_\lambda + (\mathrm{T}\otimes\mathrm{S})w''_\lambda}{2} \bar{F}(t,\theta)dtd\theta \\ &= \frac{1}{2\sqrt{\pi}} \times \frac{1}{2}\{< w''_\lambda, F > + < (\mathrm{T}\otimes\mathrm{S})w''_\lambda, F >\} \\ &= \frac{1}{2\sqrt{\pi}} < w''_\lambda, F > \end{aligned}$$

Analogously, (9) holds.

Theorem 2.1. The collection w_λ and $\tilde{w}_\lambda$ $(\lambda \in \Lambda)$ is a dual frame in $\Re$.

Proof. For $\forall F \in \Re$, we have $F \in L^2(R \otimes [0,2\pi))$. According to the property of biorthogonal basis wavelet, we have

$$A\|F\|^2_{L^2(R\otimes[0,2\pi))} \le \sum_{\lambda\in\Lambda} |< F, w''_\lambda >|^2 \le B\|F\|^2_{L^2(R\otimes[0,2\pi))} \quad (10)$$

$$B^{-1}\|F\|^2_{L^2(R\otimes[0,2\pi))} \le \sum_{\lambda\in\Lambda} |< F, \tilde{w}''_\lambda >|^2 \le A^{-1}\|F\|^2_{L^2(R\otimes[0,2\pi))} \quad (11)$$

where both A and B are constant.

Then, using Lemma 2.3, we have

$$4\pi A[F,F] \le \sum_{\lambda\in\Lambda} |2\sqrt{\pi}[F, w_\lambda]|^2 \le 4\pi B[F,F]$$

$$4\pi B^{-1}[F,F] \le \sum_{\lambda\in\Lambda} |2\sqrt{\pi}[F, \tilde{w}_\lambda]|^2 \le 4\pi A^{-1}[F,F]$$

Simplifying (10) and (11),

$$A\|F\|^2_{L^2(\Re)} \le \sum_{\lambda\in\Lambda} |[F, w_\lambda]|^2 \le B\|F\|^2_{L^2(\Re)} \quad (12)$$

$$B^{-1}\|F\|^2_{L^2(\Re)} \le \sum_{\lambda\in\Lambda} |[F, \tilde{w}_\lambda]|^2 \le A^{-1}\|F\|^2_{L^2(\Re)} \quad (13)$$

Using (4) and (5), we obtain

$$\begin{aligned} F &= \sum_{\lambda\in\Lambda} <\mathrm{F}, w''_\lambda> \tilde{w}''_\lambda = \frac{1}{\sqrt{2\pi}} \sum_{\lambda\in\Lambda} <\mathrm{F}, w''_\lambda> \tilde{w}_\lambda \\ &= \sum_{\lambda\in\Lambda} [\mathrm{F}, w_\lambda] \tilde{w}_\lambda \end{aligned} \quad (14)$$

$$\begin{aligned} F &= \sum_{\lambda\in\Lambda} <\mathrm{F}, \tilde{w}''_\lambda> w''_\lambda = \frac{1}{\sqrt{2\pi}} \sum_{\lambda\in\Lambda} <\mathrm{F}, \tilde{w}''_\lambda> w_\lambda \\ &= \sum_{\lambda\in\Lambda} [\mathrm{F}, \tilde{w}_\lambda] w_\lambda \end{aligned} \quad (15)$$

From (12), (13), (14) and (15), it is obvious that collection w_λ and $\tilde{w}_\lambda$ $(\lambda \in \Lambda)$ is a dual frame in $\Re$.

By now, we have constructed a dual frame in Radon domain $\Re$ using biorthogonal wavelet basis. As was mentioned above, we can obtain exactly a dual frame by mapping the one in Radon domain $\Re$ to $L^2(R^2)$. We call the dual frame in $L^2(R^2)$ as dual ridgelet frame.

It is worth emphasizing that one can obtain a tight ridgelet frame when orthonormal wavelet is used in the above construction. One can think of the dual ridgelet frame as an extension of the tight ridgelet frame. The element of a dual ridgelet frame, constructed by biorthogonal 7/9 wavelet, is shown in **Fig. 1**.

The orthonormal ridgelet can effectively represent two-dimension functions smooth away from straight singularity. And the key reason is that it transports the straight singularity to point singularity in Radon domain, and then deal with the resulting point singularity using Meyer wavelet. So, the effectiveness of orthonormal ridgelet to represent the straight singularity is due to the effectiveness of Meyer wavelet to represent point singularity. Note that the dual ridgelet frame is constructed in Radon Domain. As a result, we believe that the dual ridgelet frame retains the ability to effectively represent straight singularity.

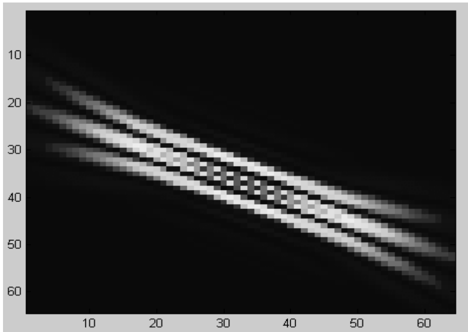

(a)

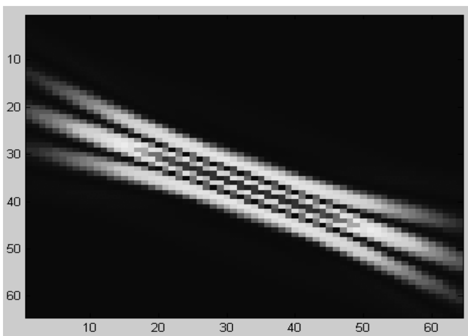

(b)

Fig. 1. Elements of dual ridgelet frame constructed by 7/9 wavelet. (a) and (b) are dual for each other

3. IMAGE DENOISING USING DUAL RIDGELET FRAME

Based on the localization principle and subband decomposition, monoscale ridgelet and curvelet were proposed [7] [8], both of which were derived from the ridgelet analysis and can efficiently deal with smooth images with smooth edges including straight and curve singularity. Ridgelet and their derivatives provide new and effective mathematic tools for image processing application, and some research work has been done to find new application for them. For example, paper [9] proposed an image denoising method based on curvelet, which achieved very high performance and were surprisingly good in visual effect. Especially, the ability of preserving line-type structure in the denoised image is striking.

It is not difficult for one to extend the dual ridgelet frame to the extension versions of monoscale ridgelet and Curvelet. And it will result in dual monoscale ridgelet frame (Dual MRF) and dual Curvelet frame. Note that the Dual MRF takes the Dual Ridgelet Frame as its basic component and constitutes a dual frame in $L^2[0,1]^2$ again [10]. In this paper, we report the performance of Dual MRF for image denoising. And we only use a simple hard threshold algorithm instead of sophisticated ones.

We carried out the experiments on Barbara of size 512×512, which is contaminated with additive Gaussian white noise with different variance levels. We compared the quality of the denoising algorithm based on Dual MRF with those based on the decimated wavelets (DWT) and undecimated wavelet (UDWT). And in our experiments, the dual monoscale ridgelet frame is constructed using biorthogonal 7/9 wavelet and the DWT and UDWT use biorthogonal 7/9 wavelet also. In **Table 1,** the PSNR of different algorithms are listed for different level noise, where the PSNR is expressed using dB.

Table 1. Comparison of image denoising algorithm based on Dual MRF with those based on wavelet in terms of PSNR on Barbara

σ /PSNR	DWT	UDWT	Dual MRF
5/34.1503	34.0345	35.9953	**36.7268**
10/28.1454	29.6963	31.7729	**33.0273**
15/24.5964	27.233	29.2088	**30.9661**
20/22.1187	25.5951	27.4093	**29.542**
25/20.1662	24.4089	26.1531	**28.4484**
30/18.5778	23.5191	25.2034	**27.6496**

From T**able 1**, it is obvious that the method based on Dual MRF outperforms substantially those based on wavelets for all noise levels.

In addition to the comparison in terms of PSNR, we display also the denoised images for visual comparison in **Fig. 2**, where the ability of Dual MRF to recover the line-type structure is well revealed. When DWT is used, artifacts blemish the resulting image seriously. In the case of using UDWT, there are few artifacts, however the line-type structures blur obviously. On the contrary, the line-type structure in image is well recovered by using the Dual MRF.

4. CONCLUSION

We have developed a new system called dual ridgelet frame in this paper, which is constructed using biorthogonal wavelet basis. And it can be considered as an extension or more general version of orthonormal ridgelet. Also, we demonstrated the high performance of the dual ridgelet frame for image denoising.

Despite of the losing of orthonormality, the dual ridgelet frame provides a more flexible tool for diverse applications in applied science, especially in image analysis and processing application. In our next paper, we will report their performances for image enhancement, classification, line detection, and etc.

5. REFERENCES

[1] M. N. Do and M. Vetterli, "Framing Pyramids," *IEEE Trans. Signal Processing*, vol. 5, pp. 2329-2342, Sep. 2003.

[2] E. L. Pennec and S. Mallat, "Image Compression with Geometrical Wavelet," in *Proc. IEEE Int. Conf. Image Processing*, Vol.1, pp. 661-664, Sept. 2000.

[3] E. J. Candès, "Harmonic Analysis of Neural Networks," *Appl. Comput. Harmon. Anal.*, vol. 6, pp. 197–218, 1999.

[4] D. L. Donoho, "Orthonormal Ridgelet and Linear Singularities," *SIAM J. Math Anal.*, vol. 31, no. 5, pp. 1062–1099, 2000.

[5] A. G. Flesia, H. Hel-Or, A. Averbuch, E. J. Candes, R. R. Coifman, and D. L. Donoho, "Digital Implementation of Ridgelet Packets," Stanford Univ., Stanford, CA, Tech. Rep., 2002.

[6] Tan Shan, L. C. Jiao, and X. C. Feng, "Ridgelet Frame," In *Proc. Int. Conf. Image Analysis and Recognition*, Porto, Springer Lecture Notes in Computer Science (LNCS) series, pp. 479-486, Sept. 2004.

[7] E. J. Candès, "Monoscale Ridgelet For the Representation of Images With Edges," Dept. Statist., Stanford Univ., Stanford, CA, Tech. Rep., 1999.

[8] E. J. Candès and D. L. Donoho, "Curvelets—A Surprisingly Effective Nonadaptive Representation for Objects With Edges," in *Curve and Surface Fitting: Saint-Malo 1999*, A. Cohen, C. Rabut, and L. L. Schumaker, Eds. Nashville, TN: Van-derbilt Univ. Press, 1999.

[9] J. L. Starck, E. J. Candès, and D.L. Donoho, "The Curvelet Transform for Image Denoising," *IEEE Trans. Image Processing*, vol. 11, pp. 670-684, June. 2002.

[10] Tanshan, and L. C. Jiao, "Monoscale Dual Ridgelet Frame: Construction and Denoising Application," submitted to *IEEE Signal Processing Letter*, 2005

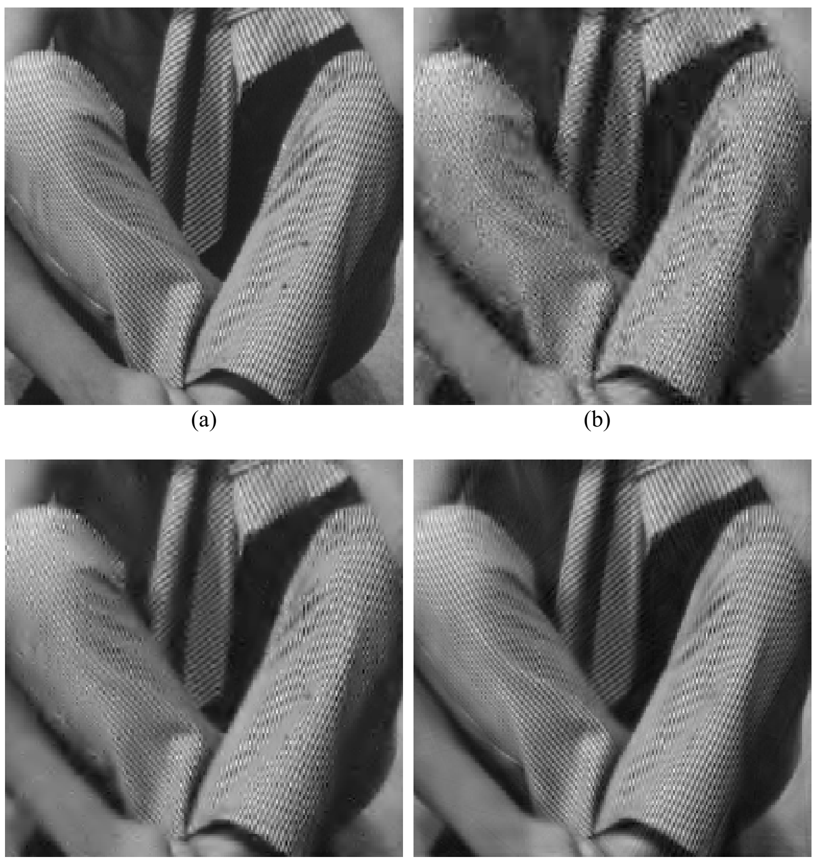

(a) (b)

(c) (d)

Fig.2. Comparison for visual effect when with white noise of standard variance 20, PSNR=22.1023, (a). Crop of original image, (b). Crop of reconstruct image using DWT, PSNR=25.5951, (c). Crop of reconstruct image using UDWT, PSNR=27.4093, (d). Crop of reconstruct image using dual ridgelet frame, PSNR=29.542